

Spacecraft Cryocooler Thermal Integration

D.L. Johnson and R.G. Ross, Jr.

**Jet Propulsion Laboratory
California Institute of California
Pasadena, CA 91109**

**Spacecraft Thermal Control Symposium
Albuquerque, New Mexico**

November 16-18, 1994

Spacecraft Cryocooler Thermal Integration

D.L. Johnson and R.G. ROSS, Jr.

Jet Propulsion Laboratory
California Institute of Technology
Pasadena, CA 91109

ABSTRACT

Spacecraft instruments requiring cryocoolers to cool infrared focal plane arrays have increased complexity in the overall design with respect to power and thermal management. The use of mechanical cryocoolers can drive spacecraft solar array and thermal radiator dimensions, and spacecraft designers must be prudent in keeping these dimensions feasible with respect to launch lift capabilities. It is important to understand cryocooler power requirements and its effects on spacecraft size and mass. Intermediate temperature (150 K to 200 K) radiators to cool radiation shields or optics on spacecraft instruments provide an as yet untapped resource for reducing the cryocooler power requirements. This paper presents cryocooler calorimetric heat rejection data and discusses the data's relationship to spacecraft thermal center; it also describes means to leverage cryocooler power requirements and thermal performance with respect to thermal heat sinking with different cryogenic radiators, and discusses their effects on spacecraft mass.

JPL has demonstrated significant thermal performance improvements to British Aerospace (BAe) cryocoolers by providing passive cooling, below 200 K along the warm end of the cryocooler coldfinger. Inclusion of the thermal strap to cool the coldfinger has resulted in 50% reductions in cryocooler input power with for the same refrigeration capacity at coldtip temperatures near 60 K. It is clearly shown in this paper that the advantages of a hybrid cooler/radiator design have profound benefits for spacecraft,

INTRODUCTION

Spacecraft instruments using infrared detectors need to maintain the detectors at a stable temperature typically between 10 K and 90 K. Mechanical cryocoolers are required to support multi-year missions, and often redundant cryocoolers are necessary to assure the overall reliability. However, the cryocooler input power required to provide the necessary cryogenic cooling requirements can severely tax the overall available spacecraft bus power. The parasitic heat load placed on operating coolers by the redundant coolers can be a substantial fraction of the available, cooling power at cryogenic temperatures if the redundant coolers are to be used without

heat switches. This parasitic heat load must be absorbed by the operating cooler, further increasing the power demands of the operating cooler. Extensive thermal design goes into the spacecraft instrument to optimize thermal heat transfer to both the spacecraft thermal radiator and to the detector system. Integration techniques such as those used by the tactical cooler community to integrate, detector and dewar to the low power cryocooler help to minimize parasitic conductive losses and increase the amount of useful cooling work that the cooler can perform, optimizing the ambient temperature heat transfer from the cooler to enable the cooler to operate as cool as possible (under the cooler's own design constraints) can potentially improve the cooler thermal performance by 10 to 20%.

This paper examines cryocooler performance sensitivities to the thermal environment provided by the spacecraft radiators. The paper draws heavily on an earlier publication describing a new spacecraft integration approach to improve the cryocooler's thermal efficiency by using a spacecraft's cryogenic-temperature passive radiator to remove heat from the cryocooler coldfinger¹. This integration concept uses a thermal link from the radiator to attach to the cryocooler coldfinger at an intermediate point along the coldfinger to intercept the parasitic heat load from the warm end of the coldfinger and 10% reduce the temperature of the gas in the regenerator. The modest amount of heat removed at the coldfinger wall has a significant effect on the measured performance of the cooler. This hybrid cryocooler/radiator design provides significant benefits in overall spacecraft design as well, which can be demonstrated in lowered electrical drive power requirements and reduced mass requirements for the spacecraft solar panel, 300-K radiator, and support structures.

The heat interceptor concept was demonstrated on two British Aerospace (BAe) coolers, the BAe 80 K and the BAe 50-80 K coolers. Incorporation of the heat interceptor was found to produce a significant thermal performance enhancement for each cooler, increasing the thermal efficiency by as much as 100%. This thermal efficiency improvement can be realized as either a reduction in cooler drive power requirements for constant cooling temperature and cooling load, or can enable a combination of lower cooling temperatures and larger cooling loads for the same drive power requirement. This is shown in the experimental results

of this paper. Before delving into the heat intercept tests, it is of use to describe the cryocooler thermal performance and heat rejection sensitivities with respect to heat sink temperatures.

CRYOCOOLER THERMAL PERFORMANCE:

The thermal efficiency of the cryocooler is dependent on the cooler body temperature, the efficiency increasing with decreasing heat sink temperature (cooler body temperature). Over the typical (0°C to 40°C) ambient temperatures of spacecraft, cooler performance can vary by 10 to 20%. Figure 1 shows the measured performance of the British Aerospace 50-80 K cooler under nominal operating conditions for varying heat sink temperatures. Isotherms are drawn between constant compressor stroke lines for each of the heat sink temperatures to show the shift in performance.

There is, however, a practical limit on how cold the cooler can operate, based on the temperature achievable with the spacecraft ambient temperature radiator, and the differential thermal contraction of the materials making up the close tolerance seals within the cooler. The importance of maintaining the lowest possible cooler body temperature drives the need for well-designed thermal paths to effectively remove the cooler-generated heat to the spacecraft radiator.

Nearly all of the cooler electrical drive power is consumed by the compressor, yet a significant fraction of the resulting thermal energy generated by the gas compression is passed via the gas transfer tube and dissipated at the displacer. For the British Aerospace coolers, this may be on the order of 20 - 35%; for the Hughes SSC cooler, this fraction may be as high as 60%. For coolers requiring 50 to 60 W of input power, the displacer may dissipate up to 35 W of heat from the gas. Figure 2 shows the heat rejection distribution from the BAe 50-80 K cooler for the case where the heat sink temperatures were identical for both the compressor and displacer. The figure also shows the total input power to the cooler, which remained relatively unchanged between the different heat sink temperatures. The compressor heat dissipation varied significantly with changing heat sink temperature, whereas the heat dissipation from the displacer was fairly insensitive to the heat sink temperature, and remained a small fraction of the overall heat dissipated from the cooler.

For the condition when the compressor and displacer heat sink temperatures are not the same, there is a sizable increase in heat dissipated at the cooler component having the lower heat sink temperature. Figure 3 shows the shift in heat dissipation for different relative heat sink temperatures for the BAe 50-80 K cooler. The heat sink temperature for the compressor and displacer are noted, in that order, by each of the heat rejection curves in the figure.

The displacer heat rejection can be particularly critical for designs where the displacer is supported off of a cryogenically-cooled optical bench; in such designs the displacer heat must either be absorbed by the optical bench (and rejected at the cryogenic temperature radiator), or separately conducted back to the overall instrument spacecraft radiator operating near 300 K. For the quantity of heat dissipated by the displacer as discussed above, it would be

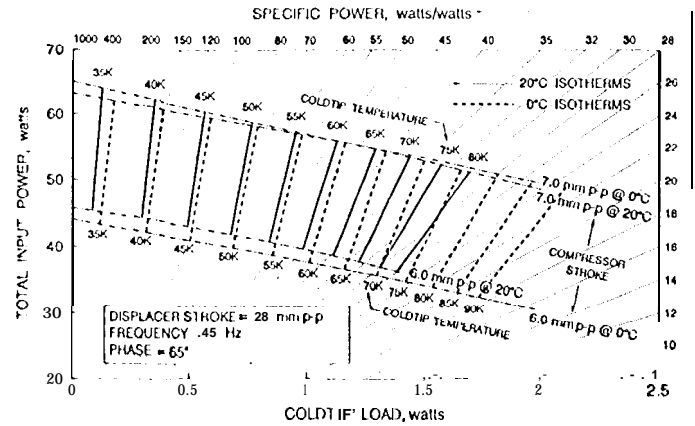


Fig. 1. BAe 50-80 K cooler thermal performance sensitivity to the heat sink temperature.

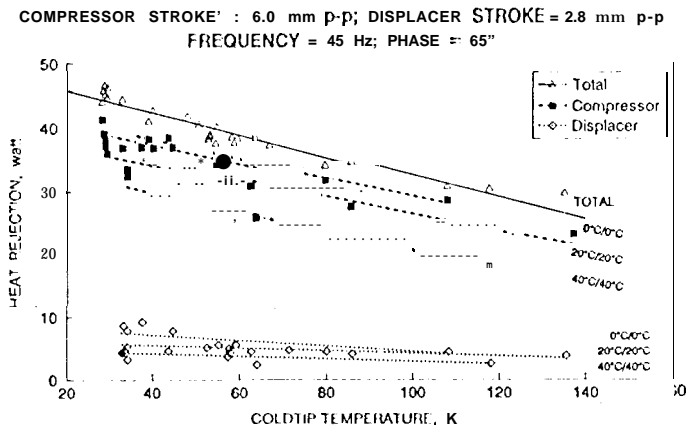


Fig. 2. Heat rejection distribution with the BAe 50-80 K compressor and displacer at the same heat sink temperature.

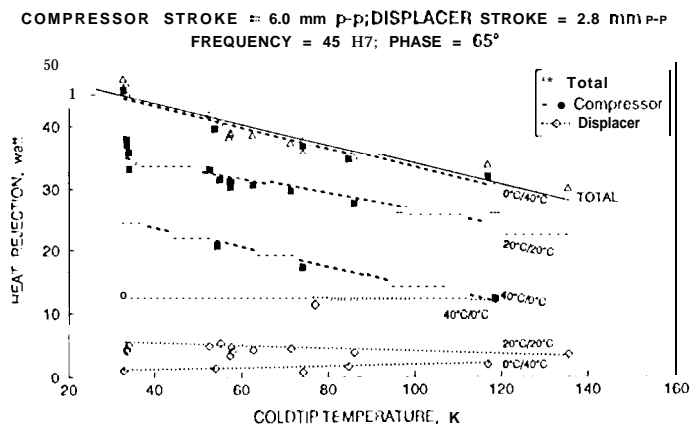


Fig. 3. Heat rejection distribution with the BAe 50-80 K compressor and displacer at unequal heat sink temperatures.

extremely difficult to reject the heat at the low temperature radiator and is therefore piped back to the 300-K spacecraft radiator. Unfortunately, the coldfinger is usually located deep

in the interior of the instrument, requiring a long massive thermal conductance link between the displacer interface flange and the 300-K spacecraft radiator. Therefore it may be desirable to maintain the displacer body temperature (heat sink temperature) at levels higher than the compressor body temperature to minimize the heat rejection from the displacer. In fact, this can be facilitated in spacecraft designs where the cryocooler compressor(s) can be located at or near the spacecraft radiator.

HEAT INTERCEPTOR PERFORMANCE

Maintaining the cooler heat sink temperatures as low as possible provides a potential 10 to 20 % performance improvement to the cryocooler. However, a much larger improvement to the cryocooler efficiency can be made by attaching a thermal strap to a point along the coldfinger and removing heat to a cold temperature sink. At this intermediate position along the coldfinger, the thermal strap intercepts the parasitic heat load from the warm end of the displacer and in addition removes a small amount of heat from the gas. Because the heat content of the gas is already much reduced at this intermediate temperature, the amount of heat removed at the coldfinger wall has a significant effect on the measured performance of the cooler.

EXPERIMENTAL MEASUREMENTS - Each of the BAe coolers was instrumented and operated in JPL's off-state thermal conductance test facility⁵. In the facility, the coldfinger is enclosed in a vacuum housing together with the coldfinger of a Gifford-McMahon (G-M) cooler, which provides the cold sink for the BAe coldfinger. The test configuration is shown in Fig. 4. The BAe compressor and displacer were mounted to heat sink plates and maintained at 20°C with the aid of a recirculating chiller to insure repeatability between tests. A flexible copper thermal strap was mechanically attached to one of the two stiffening rings machined into the BAe coldfinger, as shown in Fig. 5.

Each of the BAe coolers was initially operated at nominal compressor and displacer strokes without the thermal strap attached to the coldfinger to obtain a baseline thermal performance loadline against which the subsequent thermal performance loadlines taken with the thermal strap would be compared. The copper flange was attached to the stiffening ring to measure the temperature at the stiffening ring. Indium foil inserted between the stiffening ring and the flange insured good thermal contact. Temperature measurements were made with a silicon diode mounted to the flange. The nominal temperature at this stiffening ring during the baseline cooler operation was 250 K, and was observed to increase by 10 K over the range of coldtip loads tested. No attempt was made to maintain the stiffening ring at a constant temperature during the baseline measurements, thus the average temperature for the stiffening ring is used on the subsequent figures.

Next, the flexible copper thermal strap from the G-M cooler was attached to the flange on the stiffening ring. The heat-interceptor temperature was regulated using the G-M cryocooler together with a resistive heater on the thermal strap driven by a 110 temperature centimeter. The centimeter was capable of maintaining the stiffening ring temperature to within 0.1 K. Slow speed stick tests⁶ were run at 0.0021 Hz

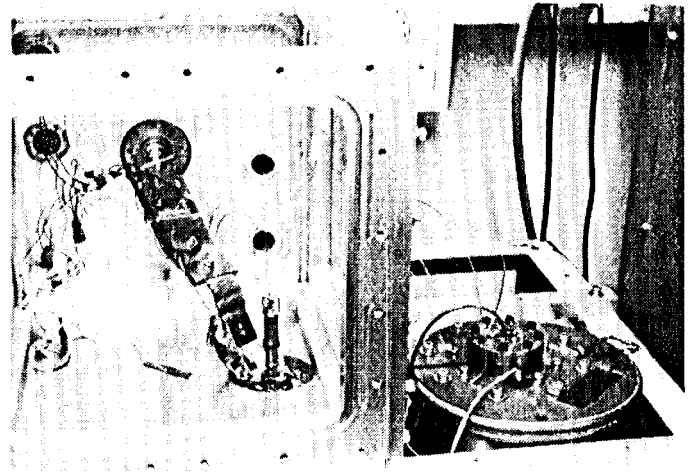


Fig. 4. Experimental test set-up for heat interceptor/cryocooler performance measurements.

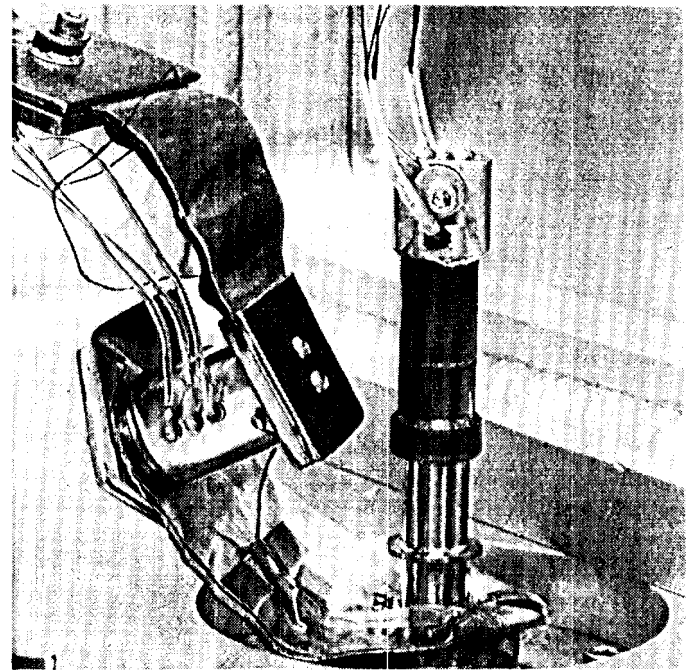


Fig. 5. Heat interceptor attachment design for coldfinger stiffening ring.

on the cold displacer to verify that the thermal strap did not put a side load onto the coldfinger sufficient to cause displacer rubbing to occur.

With the thermal strap attached to the coldfinger, thermal performance loadlines were **repeated with the same** compressor and displacer strokes as in the baseline case while maintaining the heat intercept temperature at 150 K, and then 190 K. This enabled the determination of the improvement in the thermal performance. Loadlines were also measured with reduced compressor strokes for both the 150-K and 190-K heat-intercept temperatures to determine the reduction in compressor input power possible while maintaining a constant cooling load and temperature.

Results of the loadline measurements for the BAe 80 K cryocooler **operating under the different operating conditions**

are shown in the multi-variable plot in Fig. 6. The numbers along the load-lines represent the measured coldtip temperatures at the specific coldtip loads. The solid line represents the baseline thermal performance of the cryocooler without the application of the heat interceptor to the coldfinger. All other loadlines were taken with the thermal strap attached to the coldfinger stiffening ring and maintaining a heat intercept temperature of 150 K or 190 K. This figure emphasizes the reduction in compressor input power possible when a cryogenically-cooled thermal strap is attached to the displacer coldfinger. Note that for a 61-K coldtip temperature and a 500-mW coldtip load, the inclusion of the 1 SO-K thermal strap reduced the compressor input power from 30.7 W to 14.7 W (a 52 % reduction).

Figure 7 provides a clearer representation of the enhanced coldtip performance obtainable with the heat interceptor while operating the compressor at a constant 7.2-mm compressor stroke. These loadlines show a significant improvement in the attainable coldtip temperature for any given cooling load. The loadline curves also show that for a given coldtip temperature as much as 300 mW of increased cooling capacity could be achieved with the 150-K heat intercept temperature, and that this increase in cooling capacity is accompanied by a 3-W decrease in cooler input power. For a coldtip temperature of 60 K, this results in a net performance improvement of over 75 %.

Results for the BAe 50-80 K cooler loadline measurements are shown in Figs. 8 and 9. The multi-variable plot in Fig. 8 shows the loadlines measured for the cooler operating with different compressor strokes and heat intercept temperatures. The solid line represents the baseline performance measure for the cooler. The other loadlines were obtained for the cooler with the thermal strap attached to the coldfinger. Similar to the BAe 80 K cooler, utilization of the 150-K strap while operating the BAe 50-80 K cooler at constant compressor stroke results in a nominal 10-K reduction in coldtip temperature along with a small reduction in compressor input power. For a 60-K coldtip temperature and a 1-W cooling load, the 150-K heat intercept strap reduced the compressor input power by 18 W over the baseline operation. Figure 9 shows a nominal 300-mW increase in cooling capacity when operating at the 150-K heat intercept temperature for constant compressor stroke operation of the cooler.

During the testing it was confirmed that the displacer electrical drive power, which is typically very small (cl watt), was not affected by the addition of the heat interceptor.

HEAT INTERCEPTOR CALORIMETRY MEASUREMENTS - During tests with the BAe 50-80 K cooler, a heat flow transducer was inserted into the thermal path of the heat intercept strap to measure the heat flow out of the coldfinger wall and into the heat interceptor cold sink. The results are shown in Fig. 10. For 60-K coldtip temperatures the quantity of heat removed via the 190-K heat strap was approximately 1.1 W, and for the 150-K heat strap the heat removed was approximately 1.7 W. The heat flow to the 150-K strap approaches 2 watts asymptotically for coldtip temperatures above 100 K.

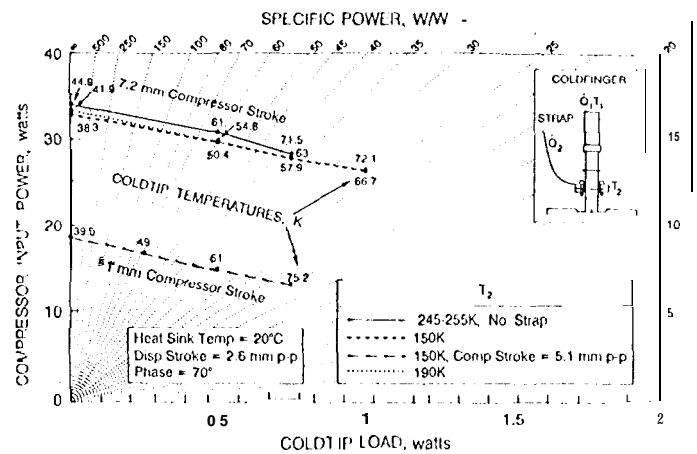


Fig. 6. Thermal performance sensitivity of BAe 80 K cooler with heat interceptor.

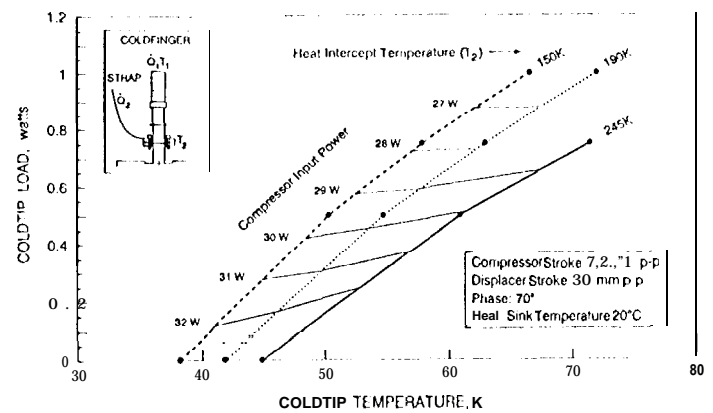


Fig. 7. Thermal performance sensitivity at constant stroke for BAe 80 K cooler with heat interceptor.

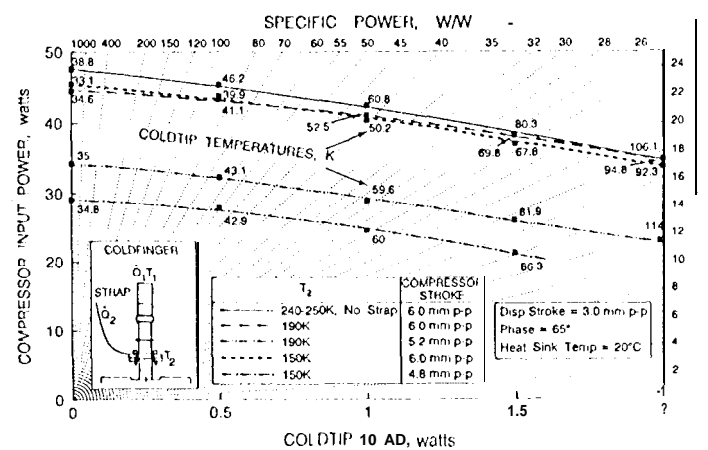


Fig. 8. Thermal performance sensitivity of BAe 50-80 K cooler with heat interceptor.

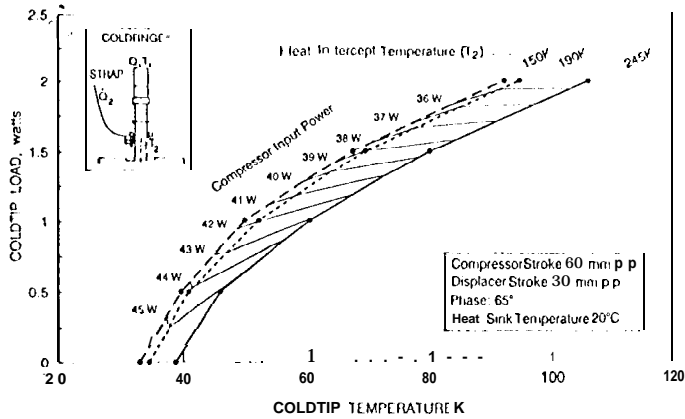


Fig. 9. Thermal performance sensitivity γ at constant stroke for BAe 50-80 K cooler with heat interceptor.

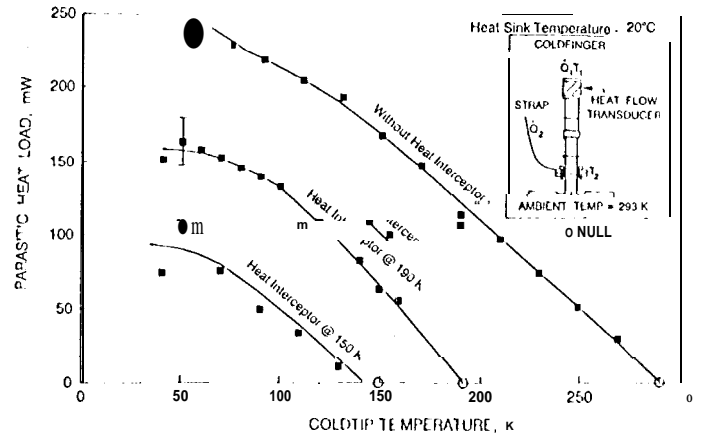


Fig. 11. BAe 50-80 K cryocooler coldfinger off-state conduction.

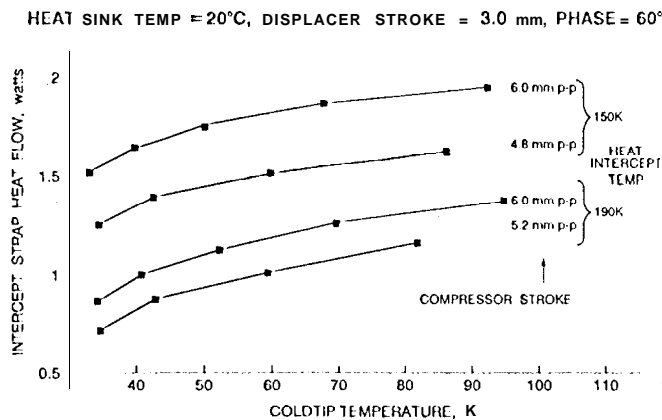


Fig. 10. Heat flow through J3Ae 50-80 K cooler heat interceptor.

COLD FINGER HEAT CONDUCTION MEASUREMENTS -Parasitic heat conduction measurements were made at the coldtip of the BAe 50-80 K cold finger to determine the change in parasitic heat load along the length of the coldfinger resulting from the attachment of the heat intercept strap. These measurements were made by adding a second G-M cooler to the vacuum chamber, its coldfinger being used to cool the coldtip of the now non-operating BAe cooler to typical flight operating temperatures. The heat flow transducer was inserted into the thermal path to measure the parasitic heat load as a function of BAe coldtip temperature. As expected, there was a significant reduction in the measured parasitic heat conduction for the cases where the heat strap was attached to the stiffening ring. The reduction, shown in Fig. 11, was as much as 150 mW at a coldtip temperature of 50 K (or about 60 %).

SPACECRAFT DESIGN IMPLICATIONS

The hybrid cooler/cryogenic radiator is applicable for both earth orbiting and deep space missions, and enables

several significant design and operational improvements for the spacecraft and the spacecraft instrument. As noted above, the incorporation of the heat intercept strap to transfer heat to a cryogenic radiator can provide significant enhancements to the cryocooler thermal performance. With a 150-K temperature heat interceptor attached to the cryocooler coldfinger, cryocooler drive power requirements can be reduced by as much as 50 %, or equally important, the 60-K refrigeration capacity of the cooler can be nearly doubled.

For spacecraft instruments which have ruled out mechanical cryocoolers because of the cryocooler input power demands, the inclusion of a cryogenic temperature radiator in the spacecraft design and utilization of the heat intercept strap may be the enabling feature-s that permit the instrument to incorporate cryocoolers to extend mission lifetimes or to enhance mission objectives. The use of the cryogenic radiator could be extended to provide cryogenic thermal shielding about the detector to reduce the radiative load on the detector. For small missions where the parasitic heat load from a redundant cooler may have been comparable to the detector cooling requirement, the utilization of the heat intercept strap would also reduce the parasitic load from the redundant cooler, making its inclusion into the overall thermal design feasible.

For low earth orbiting spacecraft, cryogenic radiators are capable of operating at temperatures around 150 K to 180 K. Radiator performance is highly orbit dependent and mission dependent, and may vary in reject temperature with each orbit or with each instrument experiment cycling on and off. Fortunately, the major enhancements in cooler performance have occurred by the time the cryogenic radiator/heat interceptor has reached 200 K, thus the operational performance of the cooler is reasonably insensitive to cryogenic radiator temperature fluctuations occurring below 200 K, as can be seen in Fig. 12.

Besides the improvement in cryocooler performance, there are significant spacecraft size and mass savings as well. To assess the potential benefits to incorporating the heat intercept concept into a spacecraft, it is useful to examine the performance improvement to the BAe 50-80 K cooler as an example. The measured performance data from Figs. 5

DISPLACER STROKE = 3.0mm, PHASE = 65°, HEAT SINK TEMPERATURE = 20°C

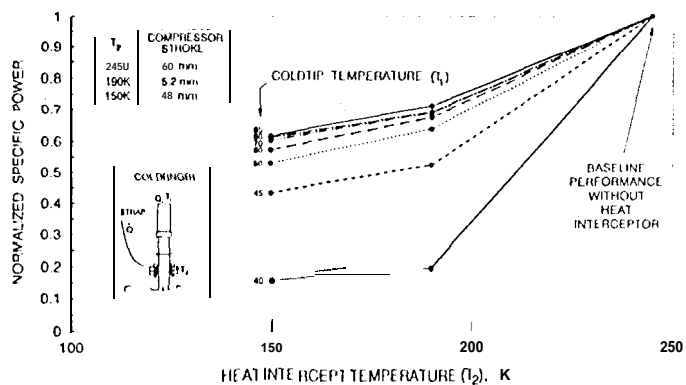


Fig. 12. Normalized cooler specific power as a function of heat intercept temperature for various isotherms.

and 7 show that operating the BAe 50-80 K cooler with the 150-K heat interceptor while applying a 1 watt refrigeration load at 60 K, results in a 18-W reduction in cooler drive power and a conduction of 1.5 W from the cold finger into the 150-K heat strap.

The 18-W reduction in electrical power results in a reduction in solar panel area. Assuming a solar panel with an efficiency of 8% for converting sunlight into electrical power, and a solar constant at earth of 1356 W/m², the solar panel electrical power productivity is approximately 110 W/m². This suggests an associated 0.164-m² reduction in solar panel area. There is an accompanying reduction in storage battery size as well (the storage battery is needed to continue the operation of the spacecraft as it passes through the earth's shadow).

The 18-W power reduction also means a 18-W reduction in heat being dissipated from the cooler to the 300-K radiator, while the 1.5 watts conducted from the heat interceptor to the cryogenic radiator will increase the size of this radiator. Assuming both the 300-K and 150-K radiators have an emissivity of 0.9 and ideally radiate to deep space, there is a resulting 0.043 m² decrease in the size of the 300-K radiator and a 0.058 m² increase in the size of the 150-K radiator.

These dimensional changes can better be assessed in terms of the mass adjustments to these components. Mass allocations typically used for the solar panel/storage batteries and for the 300-K radiator are 0.25 kg/W and 0.1 kg/W, respectively⁷. The 18-W power reduction therefore corresponds to a potential mass reduction of 4.5 kg for the solar panel and 1.8 kg for the 300-K radiator. Using a T³ ratio to estimate a corresponding 1.6-kg/W mass allocation for the 150-K radiator, the additional 1.5 W of heat rejection at 150 K would add 2.4 kg to the mass of the 150-K radiator. The net decrease in mass suggests there could be a potential reduction in mass for the support structure for the solar panel and radiator. The order of magnitude difference in the heat flux (1.5 W vs 18 W) between the 150-K thermal strap and the 300-K thermal strap (or mounting interface structure) carrying the rejected heat to the respective radiators suggests there could be considerable savings in mass there as well. Assuming, for example, that both thermal straps were made

of copper 20 cm in length and had an end to end temperature drop of 5 K, the associated change in mass would be 3.1 kg for the 300-K thermal strap and 0.26 kg for the 150-K thermal strap. The estimated mass savings is summed up in Table 1.

Table 1. Example mass savings resulting from use of 150-K heat interceptor.

Component	Mass Change
Solar Array /flattery	-4.5 kg
300 K Radiator	- 1.8 kg
150 K Radiator	+ 2.4 kg
Compressor to Radiator Thermal Conductor	- 3.1 kg
Heat Interceptor to Radiator Thermal Strap	+ 0.3 kg
S/C Support Structure	unknown
Net Mass Savings	6.7 kg

For deep space missions it is possible to reject heat at temperatures as low as 40 K. This provides the opportunity to reject heat from the coldfinger at even lower temperatures, or to reject the heat from the first stage of a two stage coldfinger. This is expected to further reduce cooler drive power requirements, potentially enabling the use of < 10-K cryocoolers for deep space missions.

A reduction in input power to the cryocooler translates into operating the cryocooler piston and/or displacer at reduced stroke. This provides another benefit to the spacecraft as it results in a reduction of the cryocooler-generated vibration and EMI levels being transmitted to the spacecraft, and as well, reduces the stress on the flexure springs which can effect the overall reliability of the cooler,

SUMMARY

The cryocooler performance sensitivities to heat sink temperatures presented above show the importance of maintaining the spacecraft ambient temperature as low as feasibly possible. It is important to note that the heat rejection distribution from the cryocooler compressor and displacer is dependent on the relative temperature differences of their respective heat sink temperatures. From a spacecraft mass perspective, it may be advantageous to maintain the displacer heat sink temperature higher than that of the compressor, even if the displacer is supported off of a cold optical bench, to reduce the size of the thermal link needed to transfer the heat from the displacer back to the ambient temperature radiator.

The heat interceptor test results presented above show the significant performance improvements with the British Aerospace cooler, as much as 100%, when incorporating the coldfinger heat interceptor. The stiffening rings on the BAe cold finger provided a convenient and near optimal attachment point for the thermal strap. Here the parasitic load along the coldfinger wall was easily intercepted and removed. It is anticipated that additional performance improvements could be made for any given heat intercept temperature through an

optimization of the regenerator matrix or by determining the optimum attachment point along the length of the cold finger. It is expected that the performance improvements may be even more profound for external regenerator displacers and pulse tubes, where the regenerator and working gas are in intimate contact with the coldfinger wall.

The utilization of the thermal heat intercept strap to transfer a modest amount of heat from the cryocooler coldfinger to the spacecraft cryogenic radiator can provide substantial thermal efficiency improvements that translate into reductions in the electrical power and mass for the spacecraft design. The hybrid cooler/cryogenic radiator can allow low power missions to now include a cryocooler into the design without a major power penalty, or to include a redundant cryocooler to prolong mission life,

ACKNOWLEDGEMENT

The work described in this paper was carried out by the Jet Propulsion Laboratory, California Institute of Technology, under a contract with the National Aeronautics and Space Administration (NASA). The financial support of JPL's Eos-AIRS instrument for the heat interceptor development and testing is graciously acknowledged. The thermal performance characterization activities reported in this paper are a subset of the Spacecraft Cooler Characterization Task sponsored by the Ballistic Missile Defense Organization through an agreement between the Air Force Phillips Laboratory and NASA. Particular credit is due E. Jetter who prepared the graphs presented herein, and to S. Leland, who manufactured the thermal strap and assembled the test setup.

REFERENCES

1. Johnson, D.L. and Ross, R. G., Jr., "Cryocooler Coldfinger Heat Interceptor", Proceedings of the 8th International Cryocooler Conference, Vail, Colorado, June 1994, Plenum Publishing Corp., New York,
2. Kotsubo, V. Y., Johnson, D. L. ... and Ross, R. G., Jr., "Calorimetric Thermal-Vacuum Performance Characterization of the BAE 80K Space Cryocooler," SAE Paper No. 929037, Proceedings of the 27th Intersociety Energy Conversion Engineering Conference, San Diego, California, August 3-7, 1992, P-2.59, Vol. 5, pp. S.101-S.107.
3. Men, G. R., Ross, R. G., Jr., and Johnson, D.L., BAE 50-80K Cryocooler Performance Characterization, JPL Internal Document D-1 1875, Jet Propulsion Laboratory, Pasadena, CA (In Publication).
4. Men, G. R., Johnson, D.L., and Ross, R.G., Jr., Hughes S S C Cryocooler Performance Characterization, JPL Internal Document D-11 864, Jet Propulsion Laboratory, Pasadena, CA (In Publication).
5. Kotsubo, V., Johnson, D. L., and Ross, R. G., Jr., "Cold-tip Off-state Conduction Loss of Miniature Stirling Cycle Cryocoolers," Adv. Cryo. Engin., Vol. 37 B (1991), pp. 1037-1043.
6. Ross, R. G., Jr., Johnson, D. L., and Sugimura, R. S., "Characterization of Miniature Stirling-cycle Cryocoolers for Space Application," Proceedings of the 6th International Cryocooler Conference, Plymouth, Massachusetts, October 25-26, 1990, DTRC-91 /002, David Taylor Research Center (1991), pp. 27-38.
7. Nast, T. C., and Murray, D.O., AIAA Paper No. 76-979, AIAA Technical Specialists Conference, Pasadena, California, October, 1976.